Nuclear Instruments and Methods in Physics Research B xxx (2017) xxx–xxx

Contents lists available at ScienceDirect

Nuclear Instruments and Methods in Physics Research B

journal homepage: www.elsevier.com/locate/nimb

Minimum detection limits and applications of proton and helium induced X-ray emission using transition-edge sensor array

M. Käyhkö [a,*], M.R.J. Palosaari [b], M. Laitinen [a], K. Arstila [a], I.J. Maasilta [d], J.W. Fowler [c], W.B. Doriese [c], J.N. Ullom [c], T. Sajavaara [a]

[a] University of Jyvaskyla, Department of Physics, P.O. Box 35, FI-40014, University of Jyvaskyla, Finland
[b] Stresstech Oy Tikkutehtaantie 1, 40800 Vaajakoski, Finland
[c] National Institute of Standards and Technology, 325 Broadway, Boulder, CO 80305, USA
[d] University of Jyvaskyla, Department of Physics, Nanoscience Center, P.O. Box 35, FI-40014, University of Jyvaskyla, Finland

ARTICLE INFO

Article history:
Received 5 August 2016
Received in revised form 30 December 2016
Accepted 21 February 2017
Available online xxxx

Keywords:
PIXE
TES
Minimum detection limit
Helium-induced X-ray emission

ABSTRACT

We have determined minimum detection limits, MDLs, for elements $14 \leqslant Z \leqslant 86$ using a transition-edge sensor array, TES array, and as a comparison using an Amptek X-123SDD silicon drift detector, SDD. This was done using a 3 MeV proton beam and a 5.1 MeV helium beam. MDLs were determined for a thin film sample on top of C substrate, and for a bulk sample containing mostly Al. Due to the higher peak-to-background ratio, lower detection limits were obtainable using the TES array for most of the elements. However, for elements $30 \leqslant Z \leqslant 45$ the performance of the TES array was not as good as the SDD performance. This is due to the limitations of the TES used at energies >10 keV. The greatest advantage of TES comes, however, when detecting low intensity peaks close to high intensity peaks. Such a case was demonstrated by measuring a fly ash with overlapping Ti, V, Ba, and Ce peaks, where minimum detection limits of V, Ba, and Ce were decreased by factor of 620, 400, and 680, respectively, compared to the SDD.

© 2017 Elsevier B.V. All rights reserved.

1. Introduction

Particle-induced X-ray emission, PIXE, is a technique capable of detecting concentrations even in parts per million level [1]. Studying small concentration levels is essential in many situations, such as when studying biological samples, atmospheric aerosols, art or archaeological objects [1]. There are many factors limiting the minimum detection limit MDL: the main elemental composition of the sample, peak-to-background ratio, detection efficiency, etc. [1].

Transition-edge sensor, TES, having wide-energy range and great energy resolution, has been demonstrated to be a good tool in X-ray spectroscopy [2,3]. Energy resolution of 3.09 eV was previously demonstrated in our setup [4], and even sub eV resolution has been demonstrated by other authors [5] for detectors operating at lower energies. Good energy resolution makes it easier to separate X-ray lines close in energy, such as Ti Kβ (4.9318 keV) and V Kα (4.9522 keV). This makes the detection of trace elements close to minor or major elements easier than with the commonly used silicon drift detectors, SDDs. On the downside, a single TES pixel is not capable of such high count rates as SDDs, the non-linear energy response adds complexity and each pixel in a TES array detector has its unique behavior.

2. Experimental methods

The measurement setup consists of array of 160 TES pixels detailed in Refs. [4,3]. Pixels are read with a time division multiplexed SQUID read-out [6]. The measurement chamber with the TES array, silicon drift detector, and sample holder as the main components is illustrated in Fig. 1. In all measurements, the refrigerator was cooled down to 65 mK with the TES array operated at 100 mK. In the analysis, 98–102 pixels were used, while 120 pixels were read. The pixels that were rejected either had some problems with the line shape, SQUID locking or the pixels did not produce any pulses.

All measurements were done with the 1.7 MV Pelletron accelerator at the University of Jyväskylä. The proton beam was produced using the Pelletron light ion source PELLIS [7], and a 3.01 MeV $^{1}H^{+}$ beam was used in all proton measurements. The He-beam was produced with Alphatross, and a 5.11 MeV $^{4}He^{2+}$ beam was used in all He measurements. The beam was focused to the sample using two

* Corresponding author.
E-mail address: marko.kayhko@jyu.fi (M. Käyhkö).

http://dx.doi.org/10.1016/j.nimb.2017.02.040
0168-583X/© 2017 Elsevier B.V. All rights reserved.

Please cite this article in press as: M. Käyhkö et al., Minimum detection limits and applications of proton and helium induced X-ray emission using transition-edge sensor array, Nucl. Instr. Meth. B (2017), http://dx.doi.org/10.1016/j.nimb.2017.02.040

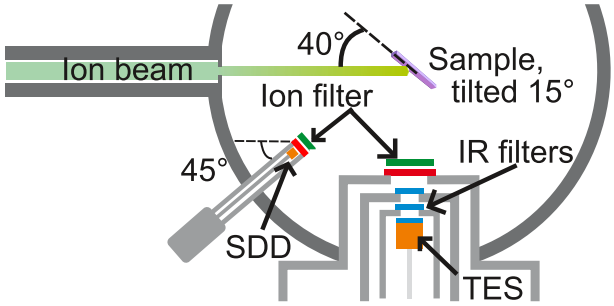

Fig. 1. A schematic view of the measurement chamber. The sample is at 40 degree angle with respect to the beam and tilted 15 degree relative to the 2D measurement plane. Transition-edge sensor array, TES, is at 90 degree angle with respect to the beam and the detector chip is 203 mm away from the sample. Silicon drift detector, SDD, is at 45 degree angle compared to the beam and the detector crystal is 199 mm away from the sample. Be filters are used in front of both detectors with 100 μm and 125 μm thicknesses for SDD, and TES, respectively. Between the sample and TES, there is also 3 infrared filters with 225 nm thick Al on 280 nm thick SiN on each, and AP3.3 vacuum window from Moxtek. Silicon drift detector has 12.5 μm thick Be window.

Table 1
Details of the performed measurements done using 3.01 MeV proton beam and 5.1 MeV He beam. The Au sample is a thin gold foil on carbon substrate manufactured by Institute for Reference Materials and Measurements, IRMM, and the certificated Au thickness was $(52.5 \pm 2.1)\mu g/cm^2$. The Al sample is manufactured by NIST, and its standard reference material number is SRM 1255b.

Sample, beam	Au, H	Al, H	Au, He	Al, He
Time, min	60	54	83	103
Cnts/pixel/s	2.97	5.62	0.46	4.16
Good pixels	100	102	98	101
Beam Q/μC	84(4)	40.8(11)	20.5(10)	35.5(10)

quadrupoles after the accelerator, and using a collimator with a 2 mm diameter located before the sample holder. A sample consisting of thin films of Ti, Cr, Cu, and Ge on a Si wafer was measured in the beginning of every measurement day to obtain an energy calibration for the TES array. The details of the measurements are given in Fig. 1 and in Table 1. The target current was not measured, and the accumulated charge was estimated using known reference materials, solid angles, detector efficiencies and X-ray yields. The estimated charges are shown in Table 1.

3. Analysis methods

3.1. Pulse-processing

All measured pulse shapes for the TES were saved and analyzed later offline. For the pulse processing, home made software was used with optimal filtering algorithm that is orthogonal to constants as described in [8]. After optimal filtering, energy calibration for each pixel was obtained using a known calibration sample containing Si, Ti, Cr, Cu, and Ge. The energy calibration is done after every cooling cycle. Due to the complex nature of the superconducting transition, a cubic spline function is fitted for every pixel. This provides a good energy calibration for the fit region, but does not extrapolate very well outside the fit region, however.

Due to small drifts in the baselines, a drift correction was used. This is mainly caused by the slight drift (10 μK) in the bath temperature of the refrigerator during long measurements. Here, a new algorithm was used for correcting the baseline drift caused by the drift in the temperature. Traditionally this is determined as

$$ph_{dc} = ph[1 + \alpha(B_j - B_0)], \tag{1}$$

where ph is the estimated pulse height, ph_{dc} is the corrected pulse height, B_0 is the baseline level in the beginning of the measurement, B_j is the baseline level for the current pulse, and α is a calibration constant for each pixel [9]. The problem we have had with this approach is that when working in a wide energy-range, the correction has not been satisfactory. The new algorithm is based on the energy calibration of the detector. Let's define a energy calibration function cal so that $E = cal(ph)$, where E is the energy of the photon hitting the detector. The drift corrected energy is calculated as

$$E_{dc} = cal(ph + \alpha \cdot \Delta) - cal(\alpha \cdot \Delta), \tag{2}$$

where $\Delta = B_j - B_0$, and α is a constant calibrated separately for each pixel. When the baseline changes by Δ, then in the energy calibration curve we move from the point Δ to $ph + \Delta$, instead of just moving from 0 to ph. When thinking about this curve in its physical meaning, the pulse height is related to the temperature of the detector. Since a pulse with height Δ and the constant drift of Δ in the base level do not have the same thermal response, a correction term α is used. In practice, it is often found that the energy calibration curve using standard cubic spline fitting can behave badly close to the zero energy. Thus, two calibration curves are used, one with a cubic spline fitting for higher energies (term $cal(ph + \alpha \cdot \Delta)$), and another, 2nd order polynomial fit for lower energies (term $cal(\alpha \cdot \Delta)$).

Pile-up pulses and other bad pulses are rejected from the analysis. Due to this, a dead time correction is needed in quantitative analysis. The dead time correction is defined by the number of accepted events divided by the number of photons arrived at the detector $\chi = N_{good}/N_{ph}$. The number of photons arrived at the detector can be approximated with the equation

$$N_{ph} \approx \frac{N_{ev}}{1 - \tau \cdot N_{ev}/T}, \tag{3}$$

where N_{ph} is the actual number of photons arrived at the detector, N_{ev} is the number of events (some with pile-up) in the saved data, τ is the recorded pulse length (16.384 ms in all measurements), and T is the measurement time as shown in Table 1. The obtained corrections for the proton beam measurements were 0.820 for the thin film sample, and 0.827 for the bulk sample. The corrections for helium beam measurements were 0.949 for the thin film sample, and 0.848 for the bulk sample.

3.2. Minimum detection limit calculations

We use the common definition for minimum detection limit yield Y_{MDL}

$$Y_{MDL} = 3\sqrt{Bg_{FWHM}}, \tag{4}$$

where Bg_{FWHM} is the background area in the full width at half maximum region [1]. This definition is valid in the situation where the peak height is much higher than the background level and the peaks are well separated [10]. The X-ray yield for a thin target can be written as

$$Y_{MDL} = Y_{it}(Z) \cdot m_{a,MDL} \cdot \gamma(Z), \tag{5}$$

where $m_{a,MDL}$ is the concentration (in g/cm^2), $Y_{it}(Z)$ is theoretical yield in unit $1/sr{\cdot}C{\cdot}g/cm^2$ containing cross sections and known physical constants, and γ is the experimental yield (in unit C·sr) calibrated using standards, containing experimental parameters like solid angle, filter transmission, and detector efficiency [1]. Now we can write

$$m_{a,MDL} = \frac{3\sqrt{Bg_{FWHM}}}{Y_{it}(Z, E_0)\gamma(Z)}. \tag{6}$$

The same equation holds for a thick target specimen, with the exception that the theoretical yield is in unit $1/str{\cdot}C{\cdot}ppm$ [1].

Please cite this article in press as: M. Käyhkö et al., Minimum detection limits and applications of proton and helium induced X-ray emission using transition-edge sensor array, Nucl. Instr. Meth. B (2017), http://dx.doi.org/10.1016/j.nimb.2017.02.040

Download English Version:

https://daneshyari.com/en/article/5467446

Download Persian Version:

https://daneshyari.com/article/5467446

Daneshyari.com